Materials Chemistry and Physics 298 (2023) 127433

Contents lists available at ScienceDirect

Materials Chemistry and Physics

journal homepage: www.elsevier.com/locate/matchemphys

Aqueous degradation and atomic layer deposition (ALD) stabilization of $BaAl_2O_4$: Eu^{2+}, Dy^{3+} long afterglow phosphors

Erkul Karacaoglu [a,d,*], Mesut Uyaner [b], Ali Kemal Okyay [c], Mark D. Losego [d,**]

[a] Metallurgy and Materials Engineering, Karamanoglu Mehmetbey University, Karaman, Turkey
[b] Aeronautical Engineering, Necmettin Erbakan University, Konya, Turkey
[c] Okyay Technologies Palo Alto, CA, USA and with the Dept. of Electrical Eng., Stanford University, CA, USA
[d] School of Materials Science and Engineering, Georgia Institute of Technology, Atlanta, GA, USA

HIGHLIGHTS

- Phosphor powder is synthesized under optimized sintering conditions via SSR method to reach single phase $BaAl_2O_4$.
- Fully aqueous degradation of $BaAl_2O_4$ host structure also induces loss in green emission of phosphor powder.
- Nanoscale metal oxide Al_2O_3 coating on phosphor particles via ALD technique can improve aqueous stability.
- The results indicate a path forward for using $BaAl_2O_4$-based phosphors in a variety of commercial applications.

ARTICLE INFO

Keywords:
$BaAl_2O_4$:Eu^{2+}
Dy^{3+}
Phosphorescence
Atomic layer deposition (ALD)
Al_2O_3 coating
Water immersion

ABSTRACT

This paper presents the aqueous degradation mechanisms of $BaAl_2O_4$:Eu^{2+}, Dy^{3+} phosphors and demonstrates an ability to prevent degradation via Al_2O_3 nano encapsulation of powders by atomic layer deposition (ALD) technique. Phosphor powder is synthesized from the solid-state reaction method. The aqueous degradation of this phosphor is systematically studied. This phosphor is found to hydrolyze and degrade within just 30 min of exposure in water. The degradation of $BaAl_2O_4$ host lattice directly affects the blue-green light emission at 497 nm, producing blue- and red-emissions that are peaked at 429 nm and 687 nm, respectively. Hydrated and structural decomposed $BaAl_2O_4$ reveals a continuous change in the phase assemblage over 30 days of immersion. To prevent this rapid degradation, use of a protective nanocoating was investigated. 10 nm Al_2O_3 coatings were applied to the surface of the phosphor powder via ALD. ALD coated $BaAl_2O_4$:Eu^{2+},Dy^{3+} phosphor retains its phosphorescence for at least 7 days of water exposure. Successful encapsulation of such phosphor particles will make them possible to use in aqueous applications or store in long-term humid environments.

1. Introduction

Persistent luminescence, or afterglow, is the phenomenon created when a phosphor material is exposed to UV-radiation or even to visible region excitation source shows visible glow in the dark for a long time, that is from minutes to tens of hours. It has long been well known that long persistent phosphors have become more useful due to their display, luminous paint (such as escape routes at airports and highways), solar cell bio-imaging, photocatalysis, photodynamic therapy, solar cell, and defense tracking applications [1,2]. These phosphors are also of interest in low-energy lighting applications. For example, light-emitting diodes (LEDs): they have taken intense attention. Their compactness, environmental friendliness long service life, and energy conservation make them more advantages than other traditional light sources which have been mostly used fluorescent and incandescent lamps, and high-intensity discharge lamps. LEDs are now widely used in almost all lighting fields including backlight sources, traffic lights, decorative lights, and automobiles [3].

It has been reported in many studies that Red (R), green (G) and blue (B) three prime color fluorescence are excited by near-ultraviolet (NUV) LEDs to create white light. Alternatively, there have been numerous studies focused green light emitting phosphors that are excited by NUV

* Corresponding author. Metallurgy and Materials Engineering, Karamanoglu Mehmetbey University, Karaman, Turkey.
** Corresponding author.
E-mail addresses: ekaracaoglu@kmu.edu.tr (E. Karacaoglu), losego@gatech.edu (M.D. Losego).

https://doi.org/10.1016/j.matchemphys.2023.127433
Received 10 June 2022; Received in revised form 23 January 2023; Accepted 25 January 2023
Available online 25 January 2023

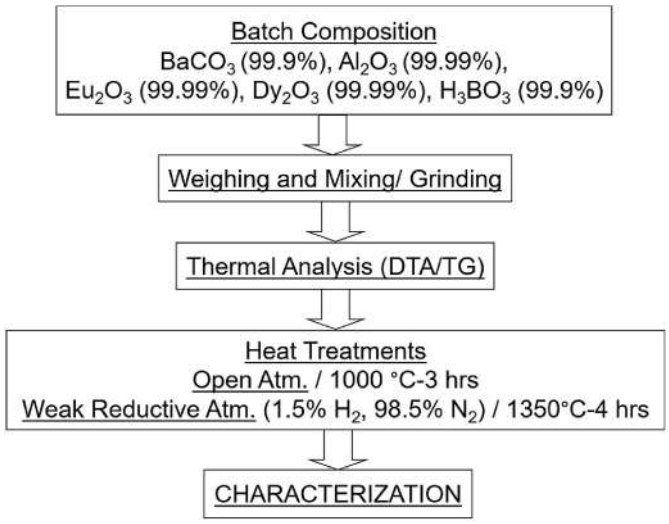

Fig. 1. Solid-state reaction synthesis process of BA2-EuDy phosphor powder.

light to provide white light. For example, sulfide-based phosphors offer high luminous efficacy and quantum efficiency, but they are likely to cause environmental pollution since they have poor chemical stability [4]. Another green emitting Eu^{2+}-doped SiAlON phosphor has high stability, yet the synthesis process is complicated and expensive [5]. The commercial applications of many phosphors are limited as in the examples given above. Another noteworthy phosphor, Eu^{2+} activated $BaAl_2O_4$ has been considered as an alternative by some researchers that has useful green emission color, low cost and facile synthesis process, and good stability [6].

The wide band gap (~4 eV) $BaAl_2O_4$ has negligible absorption in the visible region. This unique property provides minimized emission loss, thereby making it an ideal sensitizer in phosphors. The persistent luminescence of barium aluminate phosphors is mostly detected when activated and/co-doped with Eu^{2+}/Dy^{3+}, Eu^{2+}/Nd^{3+} and Ce^{3+}/Dy^{3+}. The family of stuffed tridymites which $BaAl_2O_4$ belongs have the distorted AlO_4 tetrahedral clusters share the corners which connect to form six-membered rings. In this structure, bivalent barium cations are placed inside the channels. The crystal structure of this type of phosphor can be of 5 different types depending on the lattice site. In these sites, Ba^{2+} ions are located. The Ba^{2+} ions can enter different lattice sites depending on differences in the matrix composition. Eu^{2+} activation in these host lattices provides substitution into Ba^{2+} sites, therefore the emission spectrum is influenced by these matrix elements. The replacement of Ba^{2+} (ionic radius = 1.47 *Å*) by Eu^{2+} (ionic radius = 1.25 *Å*) that depends on the Eu^{2+}: Ba^{2+} molar ratio may also modify the crystal field, further it might induce shifting the emission peaks [6–8].

Unfortunately, most barium source materials are hygroscopic, and thus susceptible to hydration that may reduce the phosphorescent performance of the material [9,10]. As far as we have observed in the studies done so far [1], we believed that a phosphor with such important phosphorescence properties should be presented in detail to what extent the photoluminescence properties are affected by the aqueous medium, as in $SrAl_2O_4$: Eu^{2+}, Dy^{3+} phosphors. In addition, the change in the photoluminescence properties of this phosphor, which has undergone structural change, that is, degradation in water, was also wanted to be presented in detail. After its behavior in water was presented in detail, there was of course a need for a process that would protect these phosphor particles from such an environment. Therefore, the particles were encapsulated with the atomic layer deposition (ALD) method in line with the experience gained from previous studies. In summary, in this paper, we examine in detail the aqueous degradation of $BaAl_2O_4$-based long afterglow phosphor powders and the implementation of ALD to coat nanoscale Al_2O_3 protective layer that improve aqueous durability. ALD has already been applied to other phosphors successfully [1,11–13], but it has never been performed to barium aluminate phosphors. ALD film thicknesses fixed at about 10 nm layer examined in this study are interrelated with light emission intensity and wavelength and have demonstrated good protection for aqueous applications.

2. Methodology

2.1. Phosphor powder synthesis

$BaAl_2O_4$:Eu^{2+},Dy^{3+} phosphor was synthesized with solid-state reaction method as summarized in Fig. 1.

Stoichiometric mixtures of high purity $BaCO_3$ (Aldrich, ≥99.9%), Al_2O_3 (Reynolds, 99.99%), Eu_2O_3, (Pacific Industrial Develeopment/ PIDC, 99.99%) and Dy_2O_3 (Aldrich, 99.99%) powder were weighed as the barium aluminate compositions of $Ba_{1-x-y}Al_2O_4$: Eu_x^{2+}, Dy_y^{3+} ($x = 0.004$, $y = 0.008$). 15 *g* of powder mixtures were homogenized with an attritor ball mill inside 100 mL jars with 50 mL isopropanol and 150 *g* of 2 mm ZrO_2 media for 4 h. After attrition, powder was dried to remove alcohol residue in a laboratory oven at 100 °C for 24 h. The heat treatment process was started with at 1000 °C for 3 h in air to decompose the $BaCO_3$ to BaO. The calcined and ground powders were sintered at 1350 °C for 4 h in a weak reducing atmosphere (98.5% N_2 and 1.5% H_2) to complete the solid state reaction. Then, single phase $BaAl_2O_4$ formation, reducing of the trivalent europium (Eu^{3+}) to its divalent state (Eu^{2+}) and achieving blue-green light emission were occurred.

2.2. Atomic layer deposition (ALD)

ALD is a vapor deposition process that stands self-limited surface reactions [11–14]. There are two sequential half-reactions on a substrate surface in this technique that is powder in this study. A metalorganic is used as the precursor and water as the co-reactant to form a metal oxide thin film on the surface of powder. The metalorganic precursor chosen in this study is trimethylaluminum (TMA, 98%, Strem Chemicals).

Conformal Al_2O_3 nano-coatings were deposited on the BA2-EuDy phosphor samples in OkyayTechALD Atomry Thermal ALD System. Silicon wafers were used in each run to follow and measure film thickness. ALD process was carried through at 150 °C for the Al_2O_3 chemistry under viscous flow conditions of 10 sccm and ~0.15–0.20 Torr Nitrogen carrier gas (99.999+% purity) with a sequencing of 15 msec precursor dose, 20 *s* purge, 15 msec H_2O dose, 20 *s* purge. This cycle was iterated until the expected film thickness was achieved. After the Al_2O_3 deposition had been reached to desired thickness on the phosphor powder for 80 cycles (~10 nm thickness), it was amorphous solid form at this process temperature [15–17].

2.3. Materials characterization methods

To determine the phases within the phosphor powders after heat treatment and water immersion, Panalytical X'Pert PRO Alpha-1 X-ray diffractometer was used that was operated at 40 kV and 40 mA (Cu-Kα radiation, λ = 1.541 *Å*) in 0.02°/2θ step-scan mode. The observation of powders' surface morphology was carried out with Hitachi SU8010 scanning electron microscope (SEM) and a LEICA DVM6 digital microscope. Thermogravimetric analysis (TGA) was achieved with PerkinElmer TGA4000. The TGA process was executed as the heating of powders in air from 25 to 900 °C (10 °C/min heating rate), holding at 900 °C for 60 min, then finally cooled back to 25 °C. The weight loss was useful to specify phosphor host lattice hydration (water content) while decomposition takes place at the same time.

Water degradation studies were performed in 25 mL cylindrical glass bottles. 2.5 *g* of the each phosphor powder was mixed in 20 mL of DI water. Powder-water mixture was then rolled horizontally on a mill at certain intervals from 30 min to 30 days to provide homogeneous

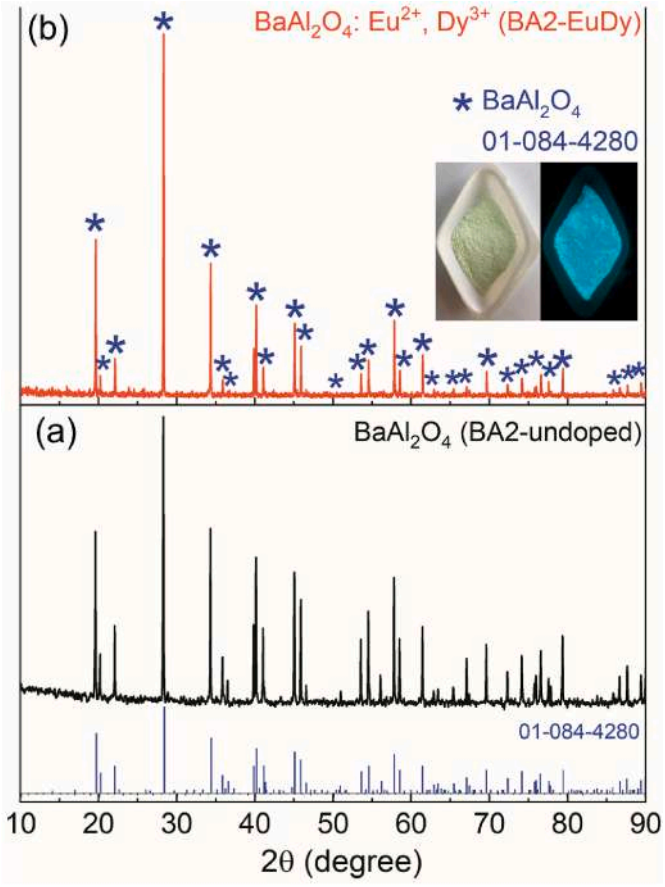

Fig. 2. XRD patterns collected from powder of (a) undoped $BaAl_2O_4$ and (b) $BaAl_2O_4$: Eu^{2+}, Dy^{3+} (BA2-EuDy). Phosphor powder were synthesized with a B_2O_3 flux. The bottom reference pattern shows peak locations for $BaAl_2O_4$ from the JCPDS file. The photographs of $BaAl_2O_4$:Eu^{2+}, Dy^{3+} powder taken in daylight and dark is placed as inset.

exposure of powder to the aqeuous medium. The pH of dispersion was continuously recorded to track decomposition byproducts. Photoluminescence (PL) properties including excitation and emission spectra of all samples were analysed at room temperature with Photon Technology International (PTI) QuantaMaster30™ Fluorescence/ Luminescence Spectrometer equipped with a 15 W Xenon CW lamp as the excitation source.

3. Results & discussion

3.1. Structural and phosphorescence analysis of as-synthesized phosphor powder

The crystal structure of undoped and doped $BaAl_2O_4$ powders were investigated with XRD. The XRD patterns given in Fig. 2 well match the powder diffraction file (JCPDS Card #01-084-4280) for the $BaAl_2O_4$ hexagonal structure, confirming that solid-state reaction synthesis was successful. The synthesized powder have a blue-green phosphorescence as given in inset image of Fig. 2. No significant diffraction peaks from secondary phases are prominent, since the radius of the Eu^{2+} (1.25 *Å*) and Dy^{3+} (1.03 *Å*) are smaller than that of Ba^{2+} (1.47 *Å*) and Ba^{2+} is substituted with rare earth ions.

3.2. Photoluminescence investigations of uncoated phosphor powder immersed in water at different time intervals

The images seen in Fig. 3 show photographs were taken in daylight and the dark environment. The images were obtained after the powders had been excited by UV-A (360 nm) light for 15 min at room temperature. It can be clearly seen from the photos that the uncoated powders lose their blue-green phosphorescence within the first 30 min of water immersion. Simultaneous with the loss in phosphorescence is an observed change in the powder's physical color and morphology, indicative of hydration.

Fig. 4 shows the comparison of PL excitation (a) and emission (b) spectra of the uncoated BA2-EuDy powder depending on water immersion time which are for 0 h, 30 min, 1 day, 3 days, 7 days, and 30 days.

The uncoated BA2-EuDy powder immediate loses blue-green emission intensity within only 30 min of water exposure. The longer the immersion time, phosphor powder has its emission maximum at 687 nm and two other emission peaks centered at 429 and 595 nm which are positioned for all water exposed samples. To understand why PL emission spectra of all powders which were immersed in water have similar and maximized at about 687 nm, we did 30 min and 1 day of water immersion studies for undoped $BaAl_2O_4$ (host) powders. The PL emission results of these two samples are given in Fig. 5(a–b).

Note that the 30 min and 1 day of water exposed undoped $BaAl_2O_4$ powders have similar emission maximums which are also similar with

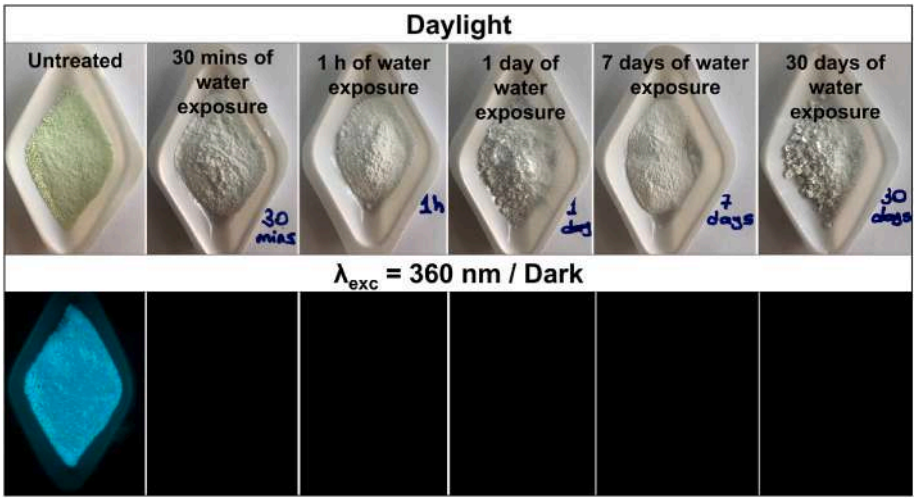

Fig. 3. Photographs in the daylight (top) and the dark (bottom) for untretaed and immersed in water at different time intervals of uncoated BA2-EuDy phosphor powder samples.

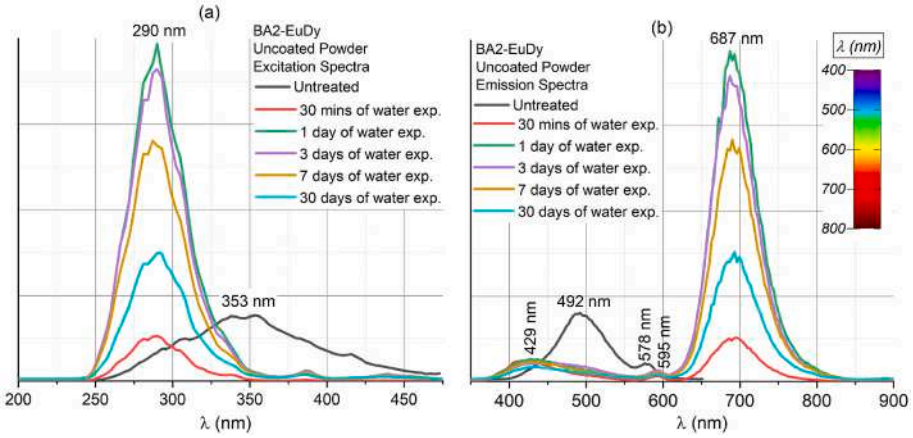

Fig. 4. Changes in PL excitation (a) and emission (b) spectra of the uncoated BA2-EuDy powder as a function of water immersion time.

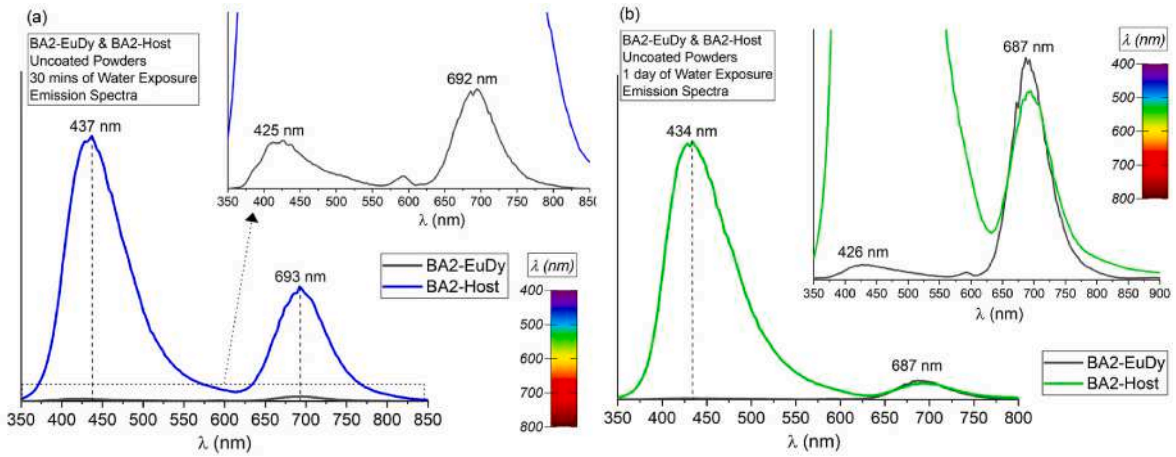

Fig. 5. Changes in PL emission spectra of the uncoated BA2-EuDy and BA2-Host powders as a function of 30 min and 1 day of water immersion time, respectively.

BA2-EuDy phosphor powder's 30 min and 1 day of water immersion results. This important finding clearly shows us the reason why BA2-EuDy phosphor powders decomposed in water within 30 min and shows completely different phosphorescence characteristics. The emission spectrum of BA2-EuDy phosphor powder obtained after 30 min of immersion in water belongs to the decomposed and hydrated $BaAl_2O_4$ host lattice which is mentioned in Phase Assemblage section given below. All phosphor powders that were exposed to 30 min no longer showed emission of Eu^{2+}-ions, but only exhibited luminescence of the degraded BA2-EuDy powder. The new blue (~430 nm) and red (~690 nm) emissions may come from newly formed electronic defect centers in the host lattices, i.e. $BaAl_2O_3(OH)_2(H_2O)$, $BaAl(OH)_5$ and $Ba_4Al_2O_7$, of both degraded BA2 (undoped) and BA2-EuDy powders. Theese emission peaks may be assigned to the intrinsic intraband gap defects within the newly formed barium aluminate phases. This is because the degradation process can induce defects, which trap electrons and holes, thus these *native defects* such as cation and anion vacancies in the host crystal causes different emission peaks. Furthermore, the PL emissions are asymmetrical, which may cause the presence of more than one cation site involved in the emission.

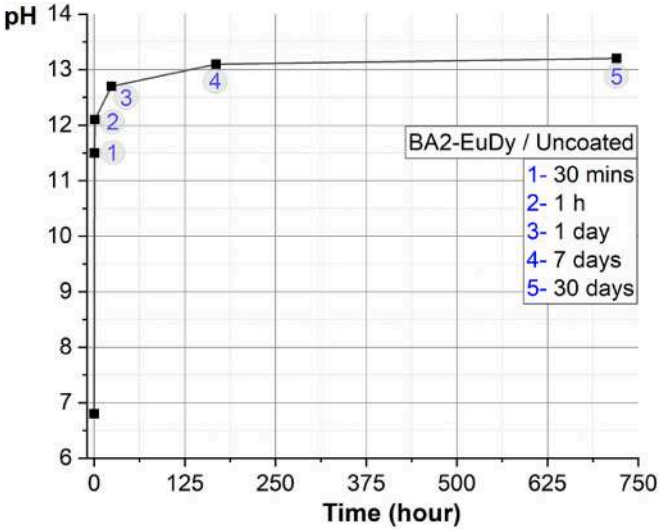

Fig. 6. Plot of the water-phosphor powder mixture pH. Note that pH changed due to species dissolution. This test was carried out for uncoated BA2-EuDy powder for up to 30 days.

3.3. Physical and chemical investigations of the $BaAl_2O_4$ degradation

3.3.1. pH of aqueous dispersion

Previous investigations of $BaAl_2O_4$-based materials have shown that these compounds can degrade by water immersion [9,10]. Based on these studies, the hydrolysis reactions of the $BaAl_2O_4$ structure with water can be shown as follows:

$$BaAl_2O_4 + H_2O \rightarrow Ba^{2+} + 2OH^- + Al(OH)_3 \downarrow$$

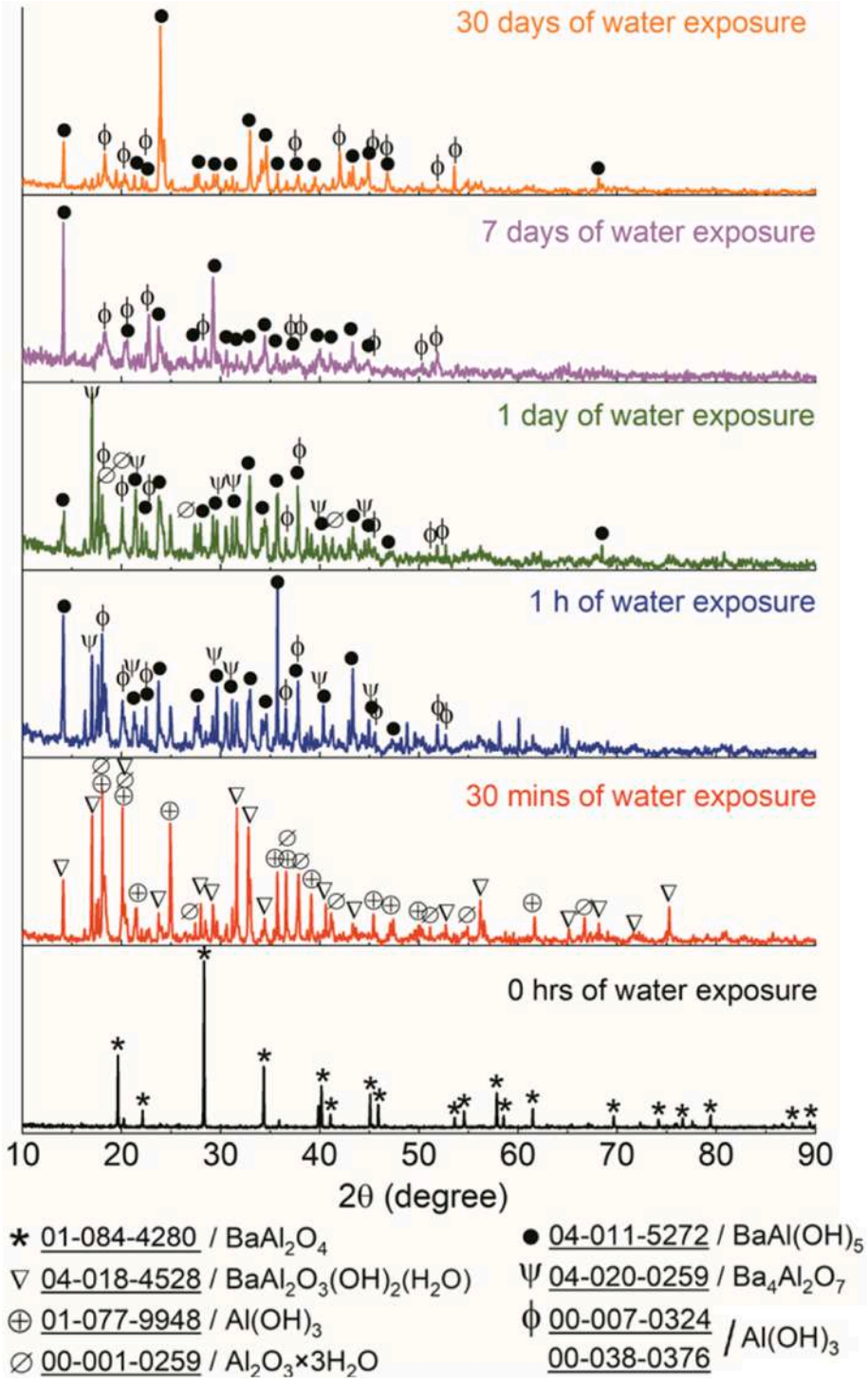

Fig. 7. Diffractograms from uncoated BA2-EuDy powder after 0 h, 30 min, 1 h, 1 day, 7 days, and 30 days of water immersion. Powders were dried in a laboratory oven at 100 °C for 24 h prior to XRD analysis.

$$BaAl_2O_4 + 2H_2O \rightarrow BaAl_2O_3(OH)_2(H_2O) \downarrow$$

$$4BaAl_2O_4 + 9H_2O \rightarrow Ba_4Al_2O_7 + 3(Al_2O_3 \bullet 3H_2O) \downarrow$$

The increase in the pH of BA2-EuDy powder in water directly depends on the formation of hydroxide ions (OH^-). As a result of increased pH of powder-water mixture, we plot Fig. 6 as a function of immersion time up to 30 days.

The increase in pH is proved evidence for the hydration of aluminate-based ceramic phosphor [18]. The uncoated phosphor powder shows a rapid rise in pH and very saturation pH which also implies the phase change.

3.3.2. Phase analysis

Fig. 7 shows the comparison of XRD patterns for water immersion of BA2-EuDy powder for 0 h, 30 min, 1 h, 1 day, 7 days, and 30 days. The water-phosphor powder mixtures were dried in a laboratory oven at 100 °C for 24 h prior to analysis.

After 30 min of water immersion, diffraction peaks of $BaAl_2O_4$ phase

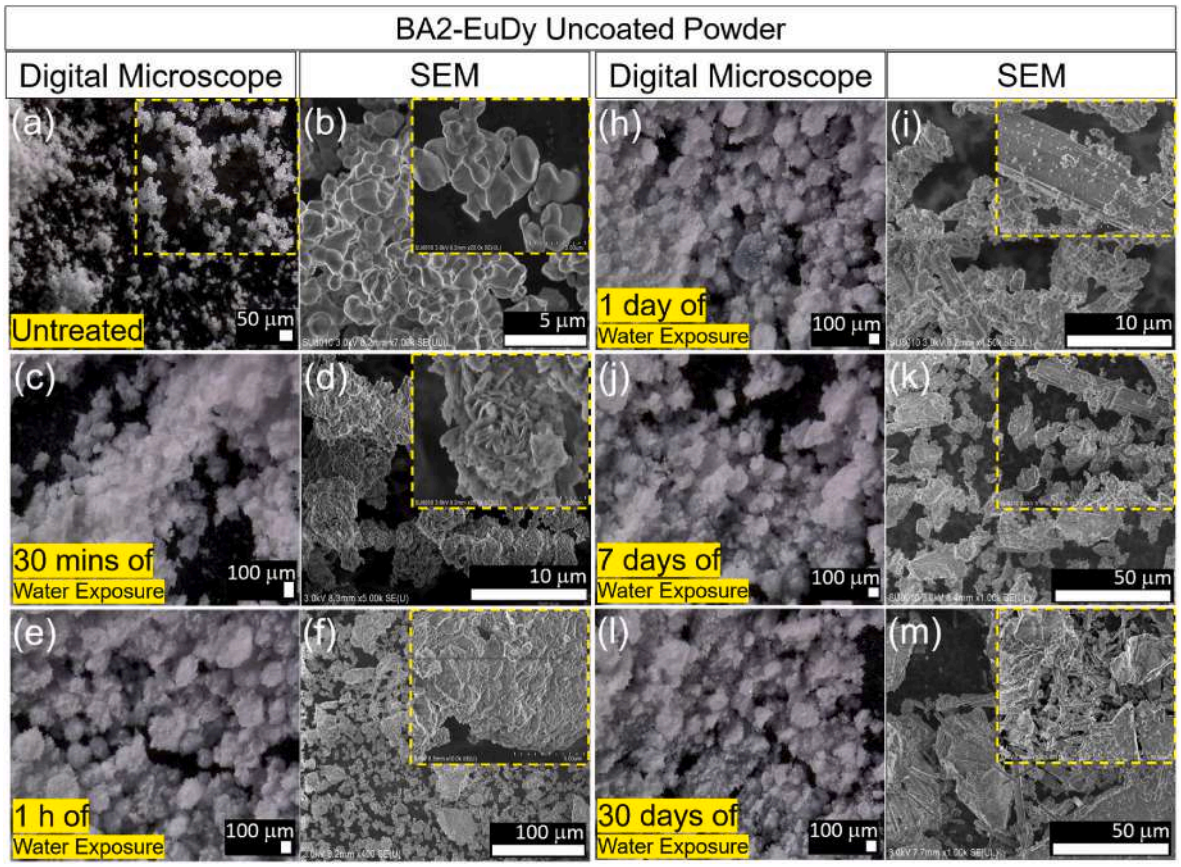

Fig. 8. Digital microscope (a, c, e, h, j, l) and SEM (b, d, f, i, k, m) images of uncoated BA2-EuDy phosphor powder prior to water exposure (a and b) and after 30 min (c and d), 1 h (e and f), 1 day (h and i), 7 days (j and k), and 30 days (l and m) of water exposure.

no longer exists, new pattern appears and is assigned to intermediate phases, i.e. $BaAl_2O_3(OH)_2(H_2O)$, $Al(OH)_3$, and $Al_2O_3{\bullet}3H_2O$. In the presence of water the hydrates were further in 1 h converted to BaAl $(OH)_5$ and $Ba_4Al_2O_7$.This phosphor powder contained phases different from those that arise when immersed for 1 h and then left for 30 min. The powder that is kept in water for 1 day has a similar pattern to the one that is kept for 1 h. A more aggressive immersion of phosphor powder was examined for 7 days and 30 days. These studies showed that although similar phases were formed during both water exposure processes, $BaAl(OH)_5$ phase became dominant at the end of 30 days.

3.3.3. *Powder morphology observation*

Particle surface morphology and size distribution images of uncoated phosphor powder for water immersion times were taken with digital and electron microscopy techniques. Fig. 8 shows digital microscope (a-*c*-e-h-j-l) and SEM (b-*d*-f-i-k-m) images of uncoated powder for untreated sample and the samples immersed in water for 30 min, 1 h, 1 day, 7 days, and 30 days.

Prior to water exposure (Fig. 8a and b) the powder has elliptical and round shaped particles of regular size distribution approximately between 0.3 µm and 2 µm. With water immersion, the particles tended to agglomerate and their physical and structural integrity deteriorated in 30 min of water exposure, as depicted in the insets of Fig. 8c and d.

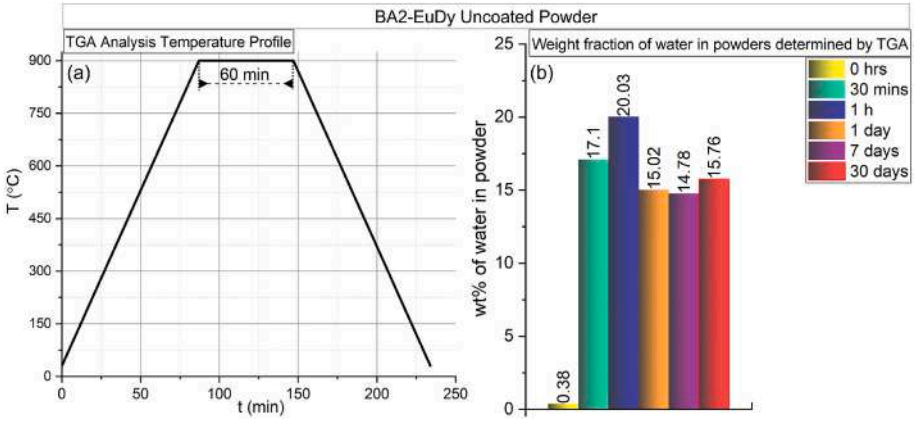

Fig. 9. (a) TGA temperature profile and (b) Weight fraction of water in powder determined by means of TGA for uncoated BA2-EuDy sample after water immersion for 0 h, 30 min, 1 h, 1 day, 7days, and 30 days.

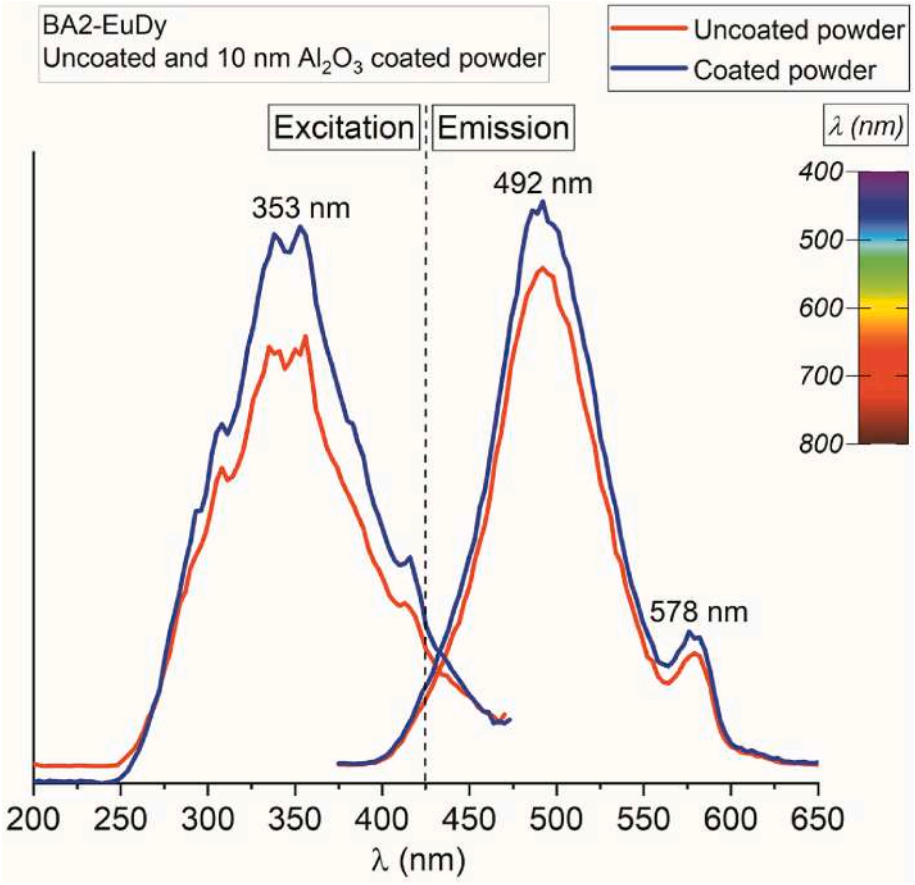

Fig. 10. PL excitation and emission spectra comparison of uncoated and 10 nm Al_2O_3 ALD coated BA2-EuDy powder.

Particles become flower shaped in 30 min of water immersion, then this formations change to irregular agglomerated particles after 1 h in water. Some particles also have regularly shaped morphologies like crystalline rods that is evidence of crystal growth (e.g., inset of Fig. 8i, k, and 8 m).

3.3.4. *Hydration*

The degree of BA2-EuDy powder hydrolysis was quantified after water immersion studies using TGA. To achieve this, the heating temperature was carried out at 900 °C for 1 h to convert all hydroxides back to oxides (Fig. 9a-b).

It was assumed that any mass loss was clearly the result of water

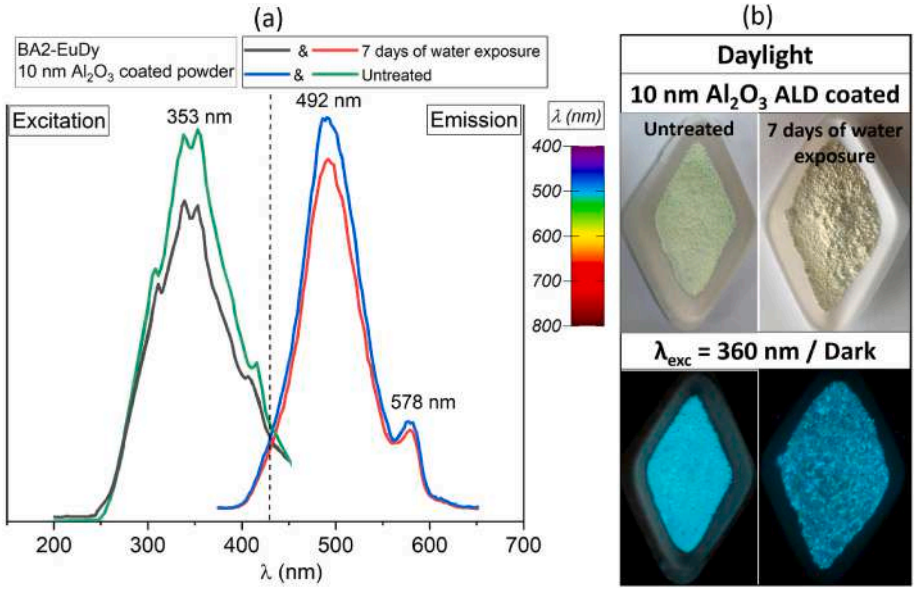

Fig. 11. Phosphorescence excitation and emission intensity change of ALD coated powder as a function of 7 days water exposure (a) and inset daylight and dark environment photographs of coated powder before and after immersion (b).

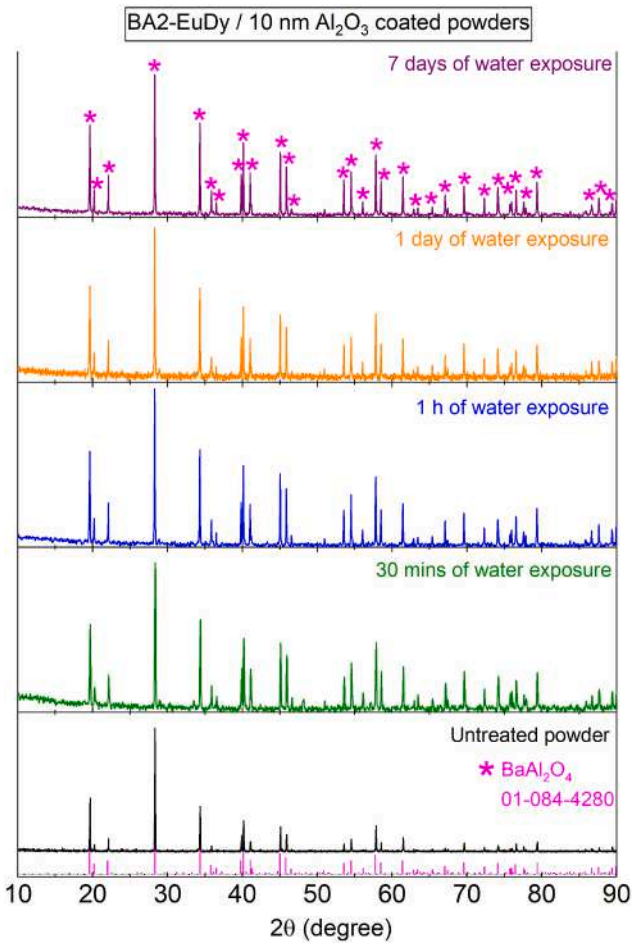

Fig. 12. Diffractograms from 10 nm Al_2O_3 coated BA2-EuDy powder after 0 h, 30 min, 1 h, 1 day, and 7 days of water immersion. Powders were dried in a laboratory oven at 100 °C for 24 h prior to XRD analysis.

removal ($M(OH)_{2x} \rightarrow MO_x + xH_2O$). Mass fraction of water that was obtained in each of the powder after 0 h, 30 min, 1 h, 1 day, 7 days and 30 days of water immersion. Initially, BA2-EuDy powder has no notable water percentage prior to immersion (0 h). In just 30 min of water exposure, the phosphor powder absorbs ~17.1 wt% water, then by 1 h it contains about 20 wt% water. The striking point here is that the water loss observed in powder kept in water for 1 h is the highest compared to the values in other time intervals, but after 1 h, the similar amount of water was lost in 1 day, 7 days and 30 days in water (~15% in average). These results are correlated with the result that the same phases are indexed according to XRD analysis in powder kept in water for 1 day, 7 days and 30 days.

3.4. Al_2O_3 Stabilization of BA2-EuDy phosphor powder via ALD encapsulation

So far, we studied the physical, structural and afterglow emission characteristics of BA2-EuDy phosphor powders in detail by immersing them in water at different time intervals. These studies have shown that $BaAl_2O_4$ is structurally sensitive to water, and this sensitivity will directly affect the luminescence properties of any phosphor in this host structure. In order to ensure the resistance of any phosphors used in this study and $BaAl_2O_4$ structure against water, the powders were coated with Al_2O_3 nano layer (10 nm) by ALD method.

3.4.1. Photoluminescence properties

Fig. 10 compares the PL excitation and emission spectra of the BA2-EuDy powder which represents uncotaed and 10 nm Al_2O_3 ALD coating.

PL excitation and emission spectra show only a modest difference in intensity after ALD encapsulation. The PL peak positions did not change after ALD coating. Emission spectrum also shows no evidence for Eu^{3+} that may emission wavelength at about 610 nm [19] after ALD process which was carried out in a heated chamber. This result showed that the ionic state of Eu is preserved, as is the case in our similar study on this subject [18]. The positive change in PL intensities of phosphor powder coated with ALD can be attributed to the following reasons: There may be slightly changes in light absorption due to coating this phosphor powder with a wide bandgap material which is Al_2O_3 (~7 eV) in this study, altering light scattering due to adding a nm layer on the particles with a different refractive index material. Uncoated and ALD coated powder have a broad excitation spectrum between 250 and 500 nm and an emission maximum at about 492 nm; additionally a distinct peak is measured at 578 nm which is attributed to $^4F_{9/2}$-$^6H_{13/2}$ transition of Dy^{3+} [20]. We assume the broad emission band includes both the Eu^{2+} and Dy^{3+} transitions related peaks that might be combined and peaked at 492 nm. Thus, this emission maximum is both attributed to a typical $4f^65\ d^1 \rightarrow 4f^7$ transition of Eu^{2+} ions [1,2,6,21] and $^4F_{9/2} \rightarrow {}^6H_{15/2}$ transition of Dy^{3+} [20], respectively. Briefly, this data suggests the ALD of powder which includes a complex process does not significantly alter the phosphorescence of this material.

Fig. 11 shows the comparison of PL excitation and emission spectra (a) and daylight/dark environment photographs of untreated, and 7 days of water exposed Al_2O_3 ALD coated phosphor powder.

Both the measurement result of the photoluminescence characteristics and the dark environment photographs of the coated and water-exposed phosphor powder showed that the ALD coating once again provided a luminescent powder with protection in an aqueous environment [18].

3.4.2. Phase analysis

Fig. 12 plots the XRD patterns for 10 nm Al_2O_3 ALD coated BA2-EuDy powder after water immersion for 30 min, 1 h, 1 day, and 7 days.

The XRD patterns of 10 nm Al_2O_3 ALD coated phosphor powder after water exposure are similar, indicating no detectable difference in crystal structure despite water exposure. Thus, the ALD encapsulation process confirms the ability for these 10 nm Al_2O_3 coating to protect these phosphor powders from hydrolysis of $BaAl_2O_4$. We reached similar results with this ALD protection in our previous study for $SrAl_2O_4$: Eu^{2+}, Dy^{3+} (SA2-Green) phosphor powder [18].

Based on this analysis, ALD encapsulation of particles shows good effectiveness in protecting the BA2-EuDy powder from hydration and rapid degradation ending after the first 30 min of water immersion.

3.4.3. SEM observations

Figs. 13 and 14 show SEM images of the ALD Al_2O_3 coated BA2-EuDy powder before and after 7 days and 30 days of water immersion, respectively.

7 days of water exposure doesn't effect the particle morpologies of ALD coated powder as depicted in Fig. 13. This is the demonstration of protected particles after 7 days of water immersion which is a good result to be able to use them in a water solution in any application. Then, we decided to test the ALD coated BA2-EuDy powder for 30 days of water exposure. As seen in Fig. 14, partial morphological change and agglomeration are detected some part of powder after 30 days of water immersion. This result may be indicative of hydration of the Al_2O_3 ALD layer which has recently been reported [22] and may suggest that alternative ALD coating chemistries, like TiO_2, should also be investigated.

4. Conclusion

In this study we report detailed on the synthesis and aqueous stability of blue-green-light emitting, long persistent $BaAl_2O_4$:Eu^{2+},Dy^{3+}

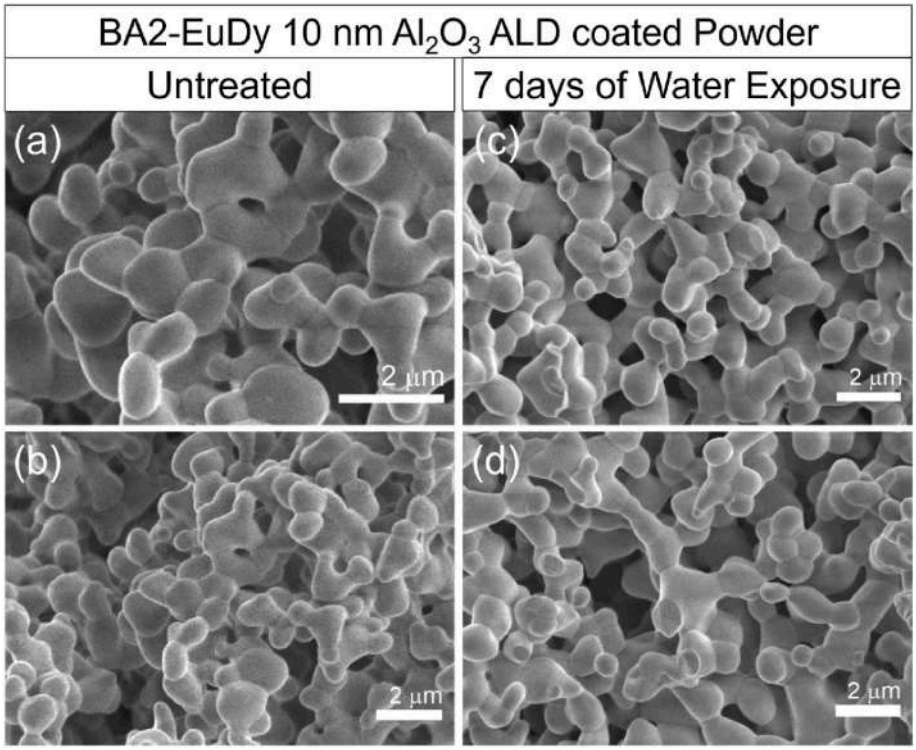

Fig. 13. SEM images of 10 nm Al_2O_3 ALD coated BA2-EuDy phosphor powder before water exposure (a and b) and after 7 days (c and d) of water exposure.

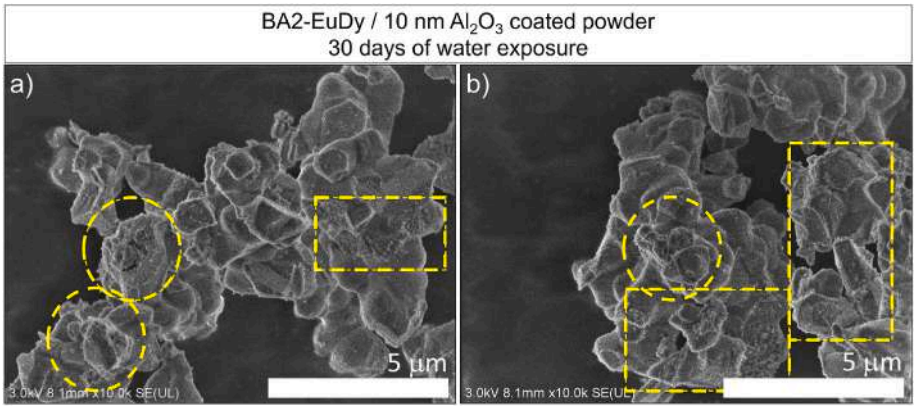

Fig. 14. SEM images of 10 nm Al_2O_3 ALD coated BA2-EuDy phosphor powder after 30 days (a and b) of water immersion. Yellow dashed rectangular and circular shapes show the partial degradation of agglomerated powder. (For interpretation of the references to color in this figure legend, the reader is referred to the Web version of this article.)

phosphor powder and how coating with nanoscale metal oxide layer that is Al_2O_3 via ALD technique can improve aqueous stability. Uncoated BA2-EuDy powder were compared along with BA2-EuDy powder ALD coated with 10 nm of Al_2O_3. Upon water immersion, uncoated powder rapidly hydrated at room temperature. This structural decomposition resulted in a loss of blue-green PL properties. In just 30 min, $BaAl_2O_4$ is hydrated easily resulting in the formation of barium aluminate hydrates and aluminum hydrate. This proves that $BaAl_2O_4$ host lattice is readily soluble in water and highly hygroscopic. XRD examinations and electron microscopy observations substantiate that the host lattice of these phosphors rapidly decompose to $BaAl(OH)_5$ and $Al(OH)_3$. However, Al_2O_3 ALD coatings can protect the phosphor for up to a week of water immersion. Even after 30 days of water immersion, phosphors are still operational, although some morphological degradation is detected. These results indicate a path forward for using BaAl2O4 based long afterglow phosphors activated with dopants like $Eu^{2+/3+}$, Dy^{3+}, Sm^{3+} or Mn^{2+} in a variety of commercial applications.

CRediT authorship contribution statement

Erkul Karacaoglu: Conceptualization, Methodology, Formal analysis, Investigation, Writing – original draft. **Mesut Uyaner:** Resources, Writing – review & editing, Supervision. **Ali Kemal Okyay:** Resources, Writing – review & editing. **Mark D. Losego:** Resources, Supervision, Validation, Writing – review & editing.

Declaration of competing interest

The authors declare the following financial interests/personal relationships which may be considered as potential competing interests: Erkul Karacaoglu reports financial support was provided by Scientific and Technological Research Council of Turkey. Erkul Karacaoglu reports

a relationship with Scientific and Technological Research Council of Turkey that includes: funding grants. Erkul Karacaoglu reports equipment, drugs, or supplies was provided by Georgia Institute of Technology. EK also would like to thank to Losego Research Group members in the School of Materials Science and Engineering at the Georgia Institute of Technology for helping with everything including laboratory uses.

Data availability

Data will be made available on request.

Acknowledgements

Erkul Karacaoglu acknowledges TUBITAK–2214-A International Doctoral Research Fellowship Programme for supporting a portion of this research to be conducted at the Georgia Institute of Technology.

References

[1] E. Karacaoglu, The Investigation of Photoluminescent and Mechanoluminescent Properties of Aluminate-Based Phosphorescence Materials Encapsulated with Atomic Layer Deposition (ALD) Method, Doctoral thesis, Selcuk University, Konya, Turkey, 2020.

[2] S. Yeşilay Kaya, E. Karacaoglu, B. Karasu, Effect of Al/Sr ratio on the luminescence properties of $SrAl_2O_4:Eu^{2+},Dy^{3+}$ phosphors, Ceram. Int. 38 (2012) 3701–3706, https://doi.org/10.1016/j.ceramint.2012.01.013.

[3] G.B. Nair, H.C. Swart, S.J. Dhoble, A review on the advancements in phosphor-converted light emitting diodes (pc-LEDs): phosphor synthesis, device fabrication and characterization, Prog. Mater. Sci. 109 (2020), 100622, https://doi.org/10.1016/j.pmatsci.2019.100622.

[4] N. Zhuo, N. Zhang, P. Chen, H. Wang, Spectral Re-absorption effect of multi-primary phosphor thin films and various package structures on the performance of near-ultraviolet white LED, ECS J. Solid State Sci. Technol. 9 (2020), 016006, https://doi.org/10.1149/2.0102001JSS.

[5] N. Hirosaki, R.-J. Xie, K. Kimoto, Characterization and properties of green-emitting β-SiAlON:Eu^{2+} powder phosphors for white light-emitting diodes, Appl. Phys. Lett. 86 (2005), 211905, https://doi.org/10.1063/1.1935027.

[6] K.A. Gedekar, S.P. Wankhede, S.V. Moharil, R.M. Belekar, d–f luminescence of Ce^{3+} and Eu^{2+} ions in $BaAl_2O_4$, $SrAl_2O_4$ and $CaAl_2O_4$ phosphors, J. Adv. Ceram. 6 (2017) 341–350, https://doi.org/10.1007/s40145-017-0246-0, 2017.

[7] L.C.V. Rodrigues, J. Hölsä, J.M. Carvalho, C.C.S. Pedroso, M. Lastusaari, M.C.F. C. Felinto, S. Watanabe, H.F. Brito, Co-dopant influence on the persistent luminescence of $BaAl_2O_4:Eu^{2+},R^{3+}$, Physica B 439 (2014) 67–71, https://doi.org/10.1016/j.physb.2013.11.007.

[8] K. Matsui, M. Arima, H. Kanno, Luminescence of barium aluminate phosphors activated by Eu^{2+} and Dy^{3+}, Opt. Mater. 35 (2013) 1947–1951, https://doi.org/10.1016/j.optmat.2012.12.002.

[9] M. Casapu, J.-D. Grunwaldt, M. Maciejewski, M. Wittrock, U. Göbel, A. Baiker, Formation and stability of barium aluminate and cerate in NOx storage-reduction catalysts, Appl. Catal. B Environ. 63 (2006) 232–242, https://doi.org/10.1016/j.apcatb.2005.10.003.

[10] L. Schoenbeck, Investigation of Reactions between Barium Compounds and Tungsten in a Simulated Reservoir Hollow Cathode Environment, Master thesis, Georgia Institute of Technology, Atlanta, US, 2005.

[11] H. Menkara, B.K. Wagner, C.J. Summers, Enhanced performance of solid-state lighting phosphors, in: Proceedings of the Seventh International Conference on Solid State Lighting, 2007 (San Diego, California, USA).

[12] N. Avci, J. Musschoot, P.F. Smet, K. Korthout, A. Avci, C. Detavernier, D. Poelman, Microencapsulation of moisture-sensitive CaS:Eu^{2+} particles with aluminum oxide, J. Electrochem. Soc. 156 (2009) J333–J337, https://doi.org/10.1149/1.3211959.

[13] R. Beetstra, U. Lafont, J. Nijenhuis, E.M. Kelder, J.R. Van Ommen, Atmospheric pressure process for coating particles using atomic layer deposition, Chem. Vap. Depos. 15 (2009) 227–233, https://doi.org/10.1002/cvde.200906775.

[14] J. Zhao, B. Gong, W.T. Nunn, P.C. Lemaire, E.C. Stevens, F.I. Sidi, P.S. Williams, C. J. Oldham, H.J. Walls, S.D. Shepherd, M.A. Browe, G.W. Peterson, M.D. Losego, G. N. Parsons, Conformal and highly adsorptive metal–organic framework thin films *via* layer-by-layer growth on ALD-coated fiber mats, J. Mater. Chem. 3 (2015) 1458–1464, https://doi.org/10.1039/C4TA05501B.

[15] X. Liang, G.D. Zhan, D.M. King, J.A. McCormick, J. Zhang, S.M. George, A. W. Weimer, Alumina atomic layer deposition nanocoatings on primary diamond particles using a fluidized bed reactor, Diam. Relat. Mater. 17 (2008) 185–189, https://doi.org/10.1016/j.diamond.2007.12.003.

[16] B.D. Piercy, C.Z. Leng, M.D. Losego, Variation in the density, optical polarizabilities, and crystallinity of TiO_2 thin films deposited via atomic layer deposition from 38 to 150 °C using the titanium tetrachloride-water reaction, J. Vac. Sci. Technol., A 35 (2017), https://doi.org/10.1116/1.4979047, 03E107.

[17] T.G. Ulusoy, A. Ghobadi, A.K. Okyay, Surface engineered angstrom thick ZnO-sheathed TiO_2 nanowires as photoanodes for performance enhanced dye-sensitized solar cells, J. Math. Chem. A. 2 (2014) 16867–16876, https://doi.org/10.1039/C4TA03445G.

[18] E. Karacaoglu, E. Ozturk, M. Uyaner, M.D. Losego, Atomic layer deposition (ALD) of nanoscale coatings on $SrAl_2O_4$-based phosphor powder to prevent aqueous degradation, J. Am. Ceram. Soc. 103 (2020) 3706–3715, https://doi.org/10.1111/jace.17041.

[19] B.M. Mothudi, O.M. Ntwaeaborwa, J.R. Botha, H.C. Swart, Photoluminescence and phosphorescence properties of $MAl_2O_4:Eu^{2+}$, Dy^{3+} (M= Ca, Ba, Sr) phosphors prepared at an initiating combustion temperature of 500°C, Physica B 404 (2009) 4440–4444, https://doi.org/10.1016/j.physb.2009.09.047.

[20] S. Chemingui, M. Ferhi, K. Horchani-Naifer, M. Férid, Synthesis and luminescence characteristics of Dy^{3+} doped $KLa(PO_3)_4$, J. Lumin. 166 (2015) 82–87, https://doi.org/10.1016/j.jlumin.2015.05.018.

[21] E. Karacaoglu, B. Karasu, The effects of re-firing process under oxidizing atmosphere and temperatures on the properties of strontium aluminate phosphors, Mater. Res. Bull. 48 (2013) 3702–3706, https://doi.org/10.1016/j.materresbull.2013.05.078.

[22] S.A. Willis, E.K. McGuinness, Y. Li, M.D. Losego, Re-examination of the Aqueous Stability of Atomic Layer Deposited (ALD) Amorphous Alumina (Al_2O_3) thin films and the use of a postdeposition air plasma anneal to enhance stability, Langmuir 37 (2021) 14509–14519, https://doi.org/10.1021/acs.langmuir.1c02574.